

## PHASE DIAGRAM OF THE SYSTEM $\text{CaF}_2$ – $\text{GdF}_3$

P. P. FEDOROV, YU. G. SIZGANOV, B. P. SOBOLEV and \*M. SHVANNER

*Institute of Crystallography, Academy of Sciences of the USSR, Moscow, USSR;*

*\*Physical Institute, Academy of Sciences of Slovakia, Bratislava, ČSSR*

(Received June 11, 1974; in revised form January 14, 1975)

A phase diagram of the system  $\text{CaF}_2$ – $\text{GdF}_3$  was studied by thermal and X-ray analysis. Two wide domains of solid solutions based on  $\text{CaF}_2$  and a high-temperature modification of  $\alpha$ - $\text{GdF}_3$  ( $\text{LaF}_3$ -structural type) are present in this system. Two maxima were found on the melting curves of the  $\text{Ca}_{1-x}\text{Gd}_x\text{F}_{2+x}$  and  $\alpha$ - $(\text{Gd}_{1-y}\text{Ca}_y)\text{F}_{3-y}$  solid solutions, at  $1428 \pm 10^\circ$  (5 mole %  $\text{GdF}_3$ ) and  $1282 \pm 5^\circ$  (85 mole %  $\text{GdF}_3$ ), respectively. The coordinates of the eutectic are 60 mole %  $\text{GdF}_3$  and  $1233 \pm 5^\circ$ .

The  $\text{CaF}_2$ – $\text{GdF}_3$  phase diagram, constructed on the basis of DTA data was reported in a previous paper [1]. Although X-ray diffraction data of annealed and quenched samples were also used, all the subsolidus phase relations in [1] were derived by supposition only. We decided to repeat the study, in order to check 1) the data of equilibria in the solid phase and 2) the unusual type of the compound  $\text{CaF}_2 \cdot 3\text{GdF}_3$  with fluorite-type structure found in [1].

### Experimental

$\text{CaF}_2$  optical single crystals (0.025 wt. % oxygen) and  $\text{GdF}_3$  powders prepared from the "000" grade oxide (0.02 wt. % oxygen, 0.003 wt. % chlorine) were used as starting reagents. DTA was carried out with the apparatus described in [2], under a highly-pure helium atmosphere. The temperature was measured with a W5Re-W2ORe thermocouple, calibrated via the melting points of  $\text{YF}_3$  [1155°, [3–5]];  $\text{HoF}_3$  [1143°, [3, 5]];  $\text{BaF}_2$  [1355° [4, 7]] and  $\text{SrF}_2$  [1463°, [4, 15]]. The weight of the samples varied from 3 to 5 g.

Thin-walled nickel or molybdenum crucible with a pocket for the thermocouple were used in the analysis. The phase transition temperatures were marked on the heating curves (heating rate  $8$ – $10^\circ/\text{min}$ ). The accuracy of the temperature determination was  $\pm 5$ – $10^\circ$ ; reproducibility  $\pm 1.5^\circ$ . Oxygen concentration in the samples after DTA was  $0.03 \pm 0.005$  wt. %.

Thermal analysis with visual-control was used for the compositions with a large percentage of  $\text{CaF}_2$ . The weight of previously-annealed samples was 240–400 mg. Melting was carried out in graphite crucibles in an atmosphere of teflon pyrolysis products. The error of the temperature determinations was  $\pm 10$ – $15^\circ$ .

Subsolidus phase equilibria were studied on samples which were equilibrated by annealing in hermetically-closed Ni-containers under an atmosphere of teflon pyrolysis products, at 610, 915, 1008 and 1067°. The annealing time varied from 2200 to 110 hours; quenching was performed with running water. X-ray control was used as to the establishment of equilibria. The oxygen concentration in the samples after this thermal treatment was 0.1–0.15 wt. %.

An AFV-202E diffractometer (Toshiba, Japan) was used for X-ray powder analysis ( $\text{CuK}_\alpha$  radiation). The lattice parameters were determined with  $\text{CaF}_2$  as an external standard ( $a = 5.46295 \text{ \AA}$  [13]). The error of such determinations for the cubic solid solutions  $\text{Ca}_{1-x}\text{Gd}_x\text{F}_{2+x}$ , which was calculated via the Student distribution, was equal to  $\pm 0.003 \text{ \AA}$ , with 99% confidence limits. The error of determination for hexagonal phase  $\alpha - (\text{Gd}_{1-y}\text{Ca}_y)\text{F}_{3-y}$  was  $\pm 0.01 \text{ \AA}$ . The equations describing the dependence of the solid solution lattice parameters on concentration were computed by the least squares method. The fit of equations to experimental data was characterized by the square standard deviations, calculated with the formula [14]:

$$S^2 = \frac{\sum_j^m n_j (\hat{y}_j - \bar{y}_j)^2}{m - q} \quad (1)$$

where  $m$  = number of compositions;

$q$  = number of calculated coefficients in the equation;

$n_j$  = number of parallel determinations for composition  $j$ ;

$\hat{y}$  = calculated value from equation; and

$\bar{y}$  = average experimental value.

Single crystals were grown by the Bridgman technique at a rate varying from 10 to 15 mm/h.

## Results and discussion

The  $\text{CaF}_2\text{--GdF}_3$  phase diagram discussed in the present study is shown in Fig. 1 and Table 1. We found the melting point of  $\text{GdF}_3$  to be  $1225 \pm 5^\circ$ , which is in good agreement with [3–5]. The transition temperature is  $1066 \pm 5^\circ$ . This coincides with the data in [3, 8], but is considerably higher than the values given in [9, 10]. It is noteworthy that on the cooling curves the same transition is recorded at lower temperatures, depending on the cooling rate. The  $\text{CaF}_2$  melting point was found to be  $1418 \pm 6^\circ$ , which coincides with the data given in [7, 11, 12].

As is seen from Fig. 1, the  $\text{CaF}_2\text{--GdF}_3$  system is a simple eutectic one, but the eutectic (60 mole %  $\text{GdF}_3$ ,  $1233^\circ$ ) is formed between two solid solutions with maxima on the melting curves. The addition of small amounts of  $\text{GdF}_3$  to  $\text{CaF}_2$  increases the melting temperature, the coordinates of the maximum being 5 mole %  $\text{GdF}_3$  and  $1428^\circ$ . This coincides with the data in [15] on the distribution coefficient

Table 1  
Thermal analysis data for the  $\text{CaF}_2\text{-GdF}_3$  system

No.	Composition, mole % $\text{GdF}_3$	Liquidus $^{\circ}\text{C}$	Solidus $^{\circ}\text{C}$	Transformation $^{\circ}\text{C}$
1	0	1418	—	—
2	3	1423	1420	—
3	7	1427	1422	—
4	10	—	1415	—
5	15	1415	—	—
6	20	1406	1382	—
7	25	1399	—	—
8	30	1368	1332	—
9	40	1333	1291	—
10	50	1290	1233*	—
11	60	1231*	1231*	—
12	67	1265	1235*	—
13	71	1274	1233*	—
14	75	1278	1265	—
15	78	1278	1270	—
16	81	1279	1272	—
17	83.5	1280	1278	—
18	87	1281	1276	—
19	89	1277	1265	—
20	92.5	1266	1248	—
21	95	1265	1227	1032
22	98	1245	1226	1061
23	100	1225	—	1066

\* eutectic

of  $\text{Gd}^{3+}$  in  $\text{CaF}_2$ , which is greater than 1. Lattice parameters of the solid solution  $\text{Ca}_{1-x}\text{Gd}_x\text{F}_{2+x}$  with a fluorite-type structure deviate substantially from Vegard's rule for specimens with a large percentage of  $\text{GdF}_3$  (Fig. 2). The concentration-dependence is given by the equation:

$$a = a_0 + 0.3202x - 0.1213x^2, \text{ \AA} \quad (2)$$

where  $x$  = mole fraction of  $\text{GdF}_3$  in  $\text{Ca}_{1-x}\text{Gd}_x\text{F}_{2+x}$ ; and

$a_0$  = lattice parameter of  $\text{CaF}_2$ , with a standard deviation of  $5.6 \cdot 10^{-6}$ .

No distortions of the fluorite structure of this solid solution have been found.

There are series of solid solutions  $\alpha\text{-(Gd}_{1-y}\text{Ca}_y\text{)F}_{3-y}$  (limit value of  $y = 0.30$  at the eutectic temperature) based on the  $\text{GdF}_3$  high-temperature modification (structural type of tysonite —  $\text{LaF}_3$ ). The solubility of  $\text{CaF}_2$  in  $\alpha\text{-GdF}_3$  is reduced by decreasing temperature: it is 24 mole % at  $917^{\circ}$ . The tysonite phase is also stable at  $610^{\circ}$ .

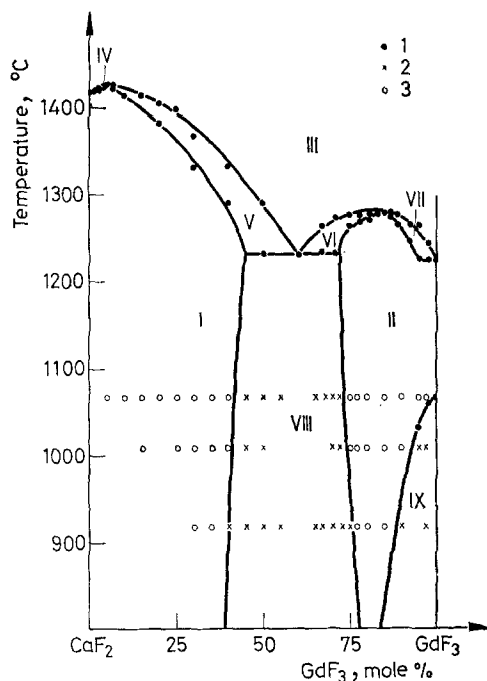


Fig. 1. Phase diagram of the  $\text{CaF}_2 - \text{GdF}_3$  system. Phase domains: I -  $\text{Ca}_{1-x}\text{Gd}_x\text{F}_{2+x}$  solid solutions; II -  $\alpha\text{-(Gd}_{1-y}\text{Ca}_y)\text{F}_{3-y}$  solid solutions; III - L (melt); IV, V - phase I + L; VI, VII - phase II + L; VIII - phase I + phase II; IX - phase II +  $\beta\text{-GdF}_3$ . 1 - data by DTA; 2 - two phases, 3 - single phase

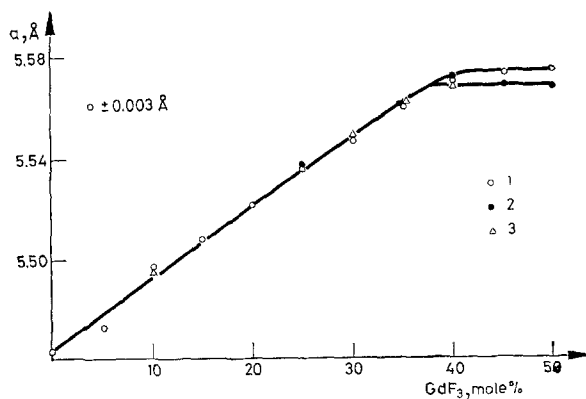


Fig. 2. Variation of lattice parameters of solid solutions  $\text{Ca}_{1-x}\text{Gd}_x\text{F}_{2+x}$  as function of  $\text{GdF}_3$  content. Determinations on samples quenched after annealing at 1:  $1067^\circ$ , 2:  $1008^\circ$ , 3:  $610^\circ$

The temperature of the  $\alpha\text{-GdF}_3$  transformation is sharply decreased by the addition of  $\text{CaF}_2$ . The thermal curves show the effect up to 5 mole %  $\text{CaF}_2$ . At the same time, the melting temperature of tysonite-type solid solutions increases, reaching a maximum value of  $1282^\circ$  at 85 mole %  $\text{GdF}_3$ . Thus, the  $\text{CaF}_2\text{-GdF}_3$  system presents a clear example of stabilization of the  $\text{LaF}_3$  structural type by the heterovalent isomorphous substitution. This phenomenon has been predicted in [16] and it was confirmed experimentally in [17, 18]. The  $\alpha\text{-GdF}_3$  modification (which is not quenched at a cooling rate of  $200\text{--}300^\circ/\text{min}$ ) stabilised by 7 mole %  $\text{CaF}_2$  may be obtained by rapid cooling and preserved for a long time at room temperature. It is noteworthy that a solid solution based on  $\alpha\text{-GdF}_3$  (concentration of  $\text{CaF}_2$  less than 5 mole %), quenched after annealing at a temperature higher than  $1066^\circ$  (that is, the  $\text{GdF}_3$  transformation point), gives a metastable solid solution with the orthorhombic structure of  $\beta\text{-GdF}_3$ . A similar phenomenon was reported in [19] for the systems  $\text{SrF}_2\text{-(Sm, Eu)F}_3$ . Variation of the lattice parameters of the hexagonal  $\alpha\text{-(Gd}_{1-y}\text{Ca}_y\text{)F}_{3-y}$  phase as a function of composition satisfies Vegard's rule and is described by the equations:

$$a = 6.893 - 0.118y, \text{ \AA} \quad (3)$$

$$c = 7.071, \text{ \AA} \quad (4)$$

Standard deviations of equations (3) and (4) are  $33 \cdot 10^{-6}$  and  $14 \cdot 10^{-6}$ , respectively.

DTA data for the  $\text{CaF}_2\text{-GdF}_3$  system given in [1] are close to ours (eutectic at 58 mole %  $\text{GdF}_2$  and  $1210^\circ$ , maximum at 75–80 mole %  $\text{GdF}_3$  and  $1300^\circ$ ). However, those authors [1] treat this diagram in another way, describing the  $\text{CaF}_2 \cdot 3\text{GdF}_3$  composition with a homogeneity field as a compound which has two modifications: high-temperature (above  $1020^\circ$ ) fluorite type, and low-temperature –  $\text{LaF}_3$  structure ( $a = 6.84$ ;  $c = 7.03 \text{ \AA}$ ). Both modifications are separated from  $\alpha\text{-GdF}_3$  by heterogeneous areas. In the present study the fluorite-like phase with a high  $\text{GdF}_3$  concentration was not found in either slowly cooled or quenched samples. These latter samples were prepared either from the melt or from a  $1067^\circ$  solid (rates of cooling were  $20\text{--}30^\circ/\text{sec}$  and  $200\text{--}300^\circ/\text{sec}$ , respectively; X-ray analysis made immediately). Long storage did not change the phase composition of these quenched samples. In tysonite-type single crystals with 75–85 mole %  $\text{GdF}_3$  this phase was not observed either. This phenomenon can be explained by the possibility of hydrolysis in the system. X-ray patterns of the quenched samples with the composition  $\text{CaF}_2 \cdot 3\text{GdF}_3$  given in [1] show a splitting of the basic fluorite (200) reflection. Such a splitting is characteristic of the tetragonal deformation of the fluorite-type structure, which is typical for the rare earth oxyfluorides. The lattice parameter of “cubic phase  $\text{CaF}_2 \cdot 3\text{GdF}_3$ ”  $a = 5.56 \text{ \AA}$  [1] is equal to the average lattice parameter of tetragonal oxyfluoride  $\text{GdO}_x\text{F}_{3-2x}$  (if  $x = 0.83$ ,  $a = 5.58$ ,  $c = 5.54 \text{ \AA}$ ) [20]. In order to verify the possibility of the hydrolysis in the  $\text{CaF}_2\text{-GdF}_3$  system the sample of the composition  $\text{CaF}_2 \cdot 4\text{GdF}_3$  (single phase with tysonite-type structure) was heated in the high-temperature

furnace of the X-ray diffractometer at  $\sim 10^{-1}$  mm Hg. A rapid hydrolysis of the sample started above  $300^\circ$ . Complete transformation of the structure was reached at  $550^\circ$ . The X-ray pattern of the new phase was similar to those for the  $\text{CaF}_2 \cdot 3\text{GdF}_3$  phase given in [1]. Determination of the pseudo cell parameter from the (311) reflection gave the value  $a = 5.55 \text{ \AA}$ . Thus, polymorphism of the  $\text{CaF}_2 \cdot 3\text{GdF}_3$  phase could be explained on the basis of the partial hydrolysis of the samples during thermal treatment.

The  $\text{CaF}_2\text{--GdF}_3$  system shown in Fig. 1 is a simple eutectic similar to the  $\text{CaF}_2\text{--LaF}_3$  system [21, 22]. Both components have a high mutual solid solubility; there are two maxima on the liquidus curve of the solid solutions.  $\text{GdF}_3$  is polymorphous.

Finally, it is worth mentioning that the phase diagram is valid at a definite oxygen concentration only, as mentioned above. It is possible that a decrease in the oxygen concentration of the samples could lead to some changes in the diagram. For example, many of the  $\text{LnF}_3$  specimens ( $\text{GdF}_3$  in particular) were not polymorphous after special treatment, was reported recently [23–25].

### Bibliographic

1. N. G. GOGADZE, E. G. IPPOLITOV and B. M. ZHIGARNOVSKII, *Zh. Neorgan. Khim.*, 17 (1972) 1152.
2. KH. S. BAGDASAROV, P. B. KALININ, J. E. LAPSKER, A. A. PRIVEZENZEV and B. P. SOBOLEV, *Zavodsk. laboratoriya*, 39 (1973) 494.
3. F. H. SPEDDING and D. C. HENDERSON, *J. Chem. Phys.*, 54 (1971) 2476.
4. B. PORPER and E. A. BROWN, *J. Am. Ceram. Soc.*, 45 (1962) 49.
5. O. N. CARLSON and F. A. SCHMIDT, *The Rare Earths*, John Wiley and Sons, Inc., New York, N. Y., 1961.
6. J. CHASSAING and D. BIZOT, *Compt. Rend., Ser. C*, 276 (1973) 679.
7. H. KOJIMA, S. G. WHITEWAY and C. R. MASSON, *Can. J. Chem.*, 46 (1968) 2968.
8. B. M. ZHIGARNOVSKII and E. G. IPPOLITOV, *Izv. Acad. Nauk. SSSR, Neorgan. Mater.*, 6 (1970) 1958.
9. R. E. THOMA and G. D. BRUNTON, *Inorg. Chem.*, 5 (1966) 1937.
10. D. A. JONES and W. A. SHAND, *J. Cryst. Growth*, 2 (1968) 361.
11. B. F. NAYLOR, *J. Am. Chem. Soc.*, 67 (1945) 150.
12. J. MUKERJI, *J. Am. Ceram. Soc.*, 48 (1965) 210.
13. R. D. ALLEN, *Amer. Miner.*, 37 (1952) 910.
14. L. P. ROOZINOV, *Statistical methods of the optimization of chemical processes*, Moscow, *Chemia*, 1972.
15. F. DELBOVE and S. LALLEMAND-CHATAIN, *Compt. Rend., Sér. C*, 270 (1970) 964.
16. M. MANSMANN, *Z. Krist.*, 122 (1965) 375.
17. L. S. GARASHINA and B. P. SOBOLEV, *Kristallografiya*, 16 (1971) 307.
18. B. P. SOBOLEV, L. S. GARASHINA, P. P. FEDOROV, N. L. TKACHENKO and K. B. SEIRANYAN, *Kristallografiya*, 18 (1973) 751.
19. O. GREIS and T. PETZEL, *Z. Anorg. Allgem. Chem.*, 403 (1974) 1.
20. K. NIHARA and S. YAJIMA, *Bull. Chem. Soc. Japan*, 44 (1971) 643.
21. E. G. IPPOLITOV, N. G. GOGADZE and B. M. ZHIGARNOVSKII, *Zh. Neorgan. Khim.*, 15 (1970) 3318.

22. R. H. NAFZIGER and N. RIAZANCE, *J. Am. Ceram. Soc.*, 55 (1972) 130.
23. M. ROBINSON, G. HILLS and D. M. CRIPE, Method for preparing high quality rare earth and alkaline earth fluoride single crystals, patent U.S.A. N 3649552.
24. R. C. PASTOR, M. ROBINSON, A. C. PASTOR and K. T. MILLER, The II Nat. Conf. on Crystal Growth, Princeton Univ. Campus, July 30, Vol. 1, p. 26, 1972.
25. R. C. PASTOR and M. ROBINSON, *Mater. Res. Bull.*, 9 (1974) 569.

RÉSUMÉ — L'étude du diagramme de phase du système  $\text{CaF}_2$ - $\text{GdF}_3$  par analyse thermique et diffraction des rayons X met en évidence deux larges domaines de solutions solides avec  $\text{CaF}_2$  et une modification haute température de  $\text{GdF}_3$  (structure type  $\text{LaF}_3$ ). On observe deux maximums sur les solidus des solutions solides  $\text{Ca}_{1-x}\text{Gd}_x\text{F}_{2+x}$  et  $\alpha\text{-(Gd}_{1-y}\text{Ca}_y\text{)F}_{3-y}$  à  $1428 \pm 10^\circ$  (5 mol%  $\text{GdF}_3$ ) et  $1282 \pm 5^\circ$  (85 mol%  $\text{GdF}_3$ ), respectivement. L'eutectique correspond à 60 mol%  $\text{GdF}_3$  et  $1233 \pm 5^\circ$ .

ZUSAMMENFASSUNG — Das Phasendiagramm des Systems  $\text{CaF}_2$ - $\text{GdF}_3$  wurde durch thermische und Röntgenanalyse untersucht. Zwei breite Gebiete von festen Lösungen beruhend auf  $\text{CaF}_2$  und einer Hochtemperaturmodifikation von  $\alpha\text{-GdF}_3$  ( $\text{LaF}_3$  Strukturtyp) sind im System zugegen. Zwei Maxima der Schmelzkurven der festen Lösungen  $\text{Ca}_{1-x}\text{Gd}_x\text{F}_{2+x}$  und  $\alpha\text{-(Gd}_{1-y}\text{Ca}_y\text{)F}_{3-y}$  wurden bei  $1428 \pm 10^\circ$  (5 Mol%  $\text{GdF}_3$ ) bzw.  $1282 \pm 5^\circ$  (85 Mol%  $\text{GdF}_3$ ) gefunden. Die Koordinaten des Eutektikums sind 60 Mol%  $\text{GdF}_3$  und  $1233 \pm 5^\circ$ .

Резюме — Изучена диаграмма состояния системы  $\text{CaF}_2$ - $\text{GdF}_3$  методами термического и рентгенофазового анализ. В системе образуются две широкие области твёрдых растворов на основе  $\text{CaF}_2$  и высокотемпературной модификации  $\alpha\text{-GdF}_3$  (структурный тип  $\text{LaF}_3$ ). На кривых плавкости твёрдых растворов  $\text{Ca}_{1-x}\text{Gd}_x\text{F}_{2+x}$  и  $\alpha\text{-(Gd}_{1-y}\text{Ca}_y\text{)F}_{3-y}$  имеются максимумы с координатами  $1428^\circ \pm 10$  (5 мол.%  $\text{GdF}_3$ ) и  $1282 \pm 10^\circ$  (85 мол.%  $\text{GdF}_3$ ) соответственно. Положение эвтектики — 60 мол.%  $\text{GdF}_3$  и  $1233 \pm 5^\circ$ .